

Application of Aphrodite3D coastal simulation Software to generate high-resolution nearshore current circulation and seabed evolution

Kapopoulos Ch.¹

¹ Aquaterra Engineering Company, 5. Gounari str., Patras Greece

*corresponding author: Kapopoulos Christoforos

e-mail: info@aquaterra.gr, ckapop@hotmail.com

Abstract. Prediction of current flow and sediment transport is important in coastal engineering especially in applications related to coastal protection and erosion control Projects. Furthermore they become significant in various other engineering applications related to wastewater management, pollution control, coastal infrastructure design, scour protection, dredging, beach restoration etc. In most cases prediction of coastal morphology and shoreline evolution is necessary in Environmental Impact Assessments for human interventions along the coast. The purpose of this paper is to present wave-generated current flow and coastal morphology patterns based on 2D model simulations with coupled depth-averaged continuity and momentum equations. High-resolution simulations on coastal hydrodynamics are generated with Aphrodite3D Software to produce representative results in an arbitrary coastal shoreline and seabed morphology. Only the two-dimensional module is presented. The model uses orthogonal grid with a small grid spacing to efficiently simulate the horizontal flow field and sediment transport in two dimensions. Different options in seabed slope and cross-shore morphology are examined. Short-term shoreline and seabed changes can be predicted from this model. Medium-term morphology can be predicted running the model's equations using coarser grid with corresponding larger time-steps.

Keywords: Coastal Simulation, numerical model, coastal erosion, coastal morphology, sediment transport

1. Introduction

Current flow and Sediment transport are important in coastal engineering applications. During the years several coastal modeling software packages are available on coastal hydrodynamics and sediment transport applications although their resolution is poor for small scale and medium scale engineering applications. Morphological changes nearshore as well as near coastal structures are often neglected during the design procedure due to the inability of most software packages to predict small scale morphological changes.

Aphrodite2D software uses the 2D continuity and momentum flow equations in a high-resolution numerical grid providing options of using either the finite-difference

or the finite volume numerical methods. High-resolution coastal hydrodynamics and sediment transport nearshore results are generated where most coastal structures are installed.

The model used is two-dimensional, vertically integrated. The bed stress calculation is based on the mean current. The computational requirements are small compared with a full three-dimensional model.

2. Hydrodynamic model

2.1. Vertically integrated equations

Mathematical description of tide and wave currents requires the simultaneous solution of the momentum equations and the unsteady continuity equations. Vertical accelerations are assumed negligible, pressure is hydrostatic over the depth, fluid density is homogenous. The two-dimensional depth averaged nonlinear equations can be written as follows:

$$\begin{aligned} \frac{\partial \eta}{\partial t} + \frac{\partial}{\partial x}(h + \eta)U + \frac{\partial}{\partial y}(h + \eta)V &= 0 \\ \frac{\partial U}{\partial t} + U \frac{\partial U}{\partial x} + V \frac{\partial U}{\partial y} \\ &= -g \frac{\partial \eta}{\partial x} - \frac{1}{\rho} \frac{\partial Pa}{\partial x} + \frac{\tau_{sx} - \tau_{bx}}{\rho(h + \eta)} - \frac{\partial S_{xx} + \partial S_{xy}}{\rho(h + \eta)} + v_h \nabla^2 U \\ \frac{\partial V}{\partial t} + U \frac{\partial V}{\partial x} + V \frac{\partial V}{\partial y} \\ &= -g \frac{\partial \eta}{\partial y} - \frac{1}{\rho} \frac{\partial Pa}{\partial y} + \frac{\tau_{sy} - \tau_{by}}{\rho(h + \eta)} - \frac{\partial S_{xy} + \partial S_{yy}}{\rho(h + \eta)} + v_h \nabla^2 V \end{aligned}$$

where t is the time, U, V are the mean vertically averaged velocities in the x and y directions, η is the free water surface elevation above mean level, g the acceleration due to gravity, h the depth below mean water level, ρ the water density, Pa the atmospheric pressure, τ_{sx} and τ_{sy} are components of surface wind stress in x and y directions, τ_{bx} and τ_{by} are components of bottom shear stress, v_h the horizontal eddy viscosity coefficient and ∇^2 the horizontal Laplacian operator.

The surface wind stresses are given by

$$\tau_{sx} = \rho_a C_{da} |V10|/V10_x \quad \tau_{sy} = \rho_a C_{da} |V10|/V10_y$$

where $|V10|$ is the wind velocity at 10m above water level, $V10_x$ and $V10_y$ are the components in x, y directions, ρ_a is the density of air, C_{da} is the wind drag coefficient. The bed stress is determined from the bottom current using a quadratic equation (Davies, 1988; Davies and Jones, 1993)

$$\tau_{bx} = \rho k u_b (u_b^2 + v_b^2)^{0.50} \quad \tau_{by} = \rho k v_b (u_b^2 + v_b^2)^{0.50}$$

where u_b and v_b are the bottom currents in x, y directions and k a dimensionless coefficient of bottom friction.

Radiation Stresses can be calculated using the simplified approach of the known formulas

$$S_{xx} = \frac{E}{2} (2n - 1) + E n \cos^2 a$$

$$S_{yy} = \frac{E}{2} n \sin(2a)$$

$$S_{xy} = \frac{E}{2} (2n - 1) + E n \sin^2 a$$

where E is the wave energy density, a the angle of incoming waves and

$$n = \frac{1}{2} \left(1 + \frac{2kd}{\sinh(2kd)} \right)$$

2.2. Seabed and Shoreline evolution

The seabed morphology is calculated from the sediment transport formula (Leont'yev, 1996)

$$\frac{\partial z_b}{\partial t} = -\frac{\partial}{\partial x} \left(q_x - 2|q_x| \frac{\partial z_b}{\partial x} \right) - \frac{\partial}{\partial y} \left(q_y - 2|q_y| \frac{\partial z_b}{\partial y} \right)$$

where z_b is the local increase of the seabed and q_x, q_y are the sediment transport rates in the longshore and cross-shore directions respectively in relation to the sediment transport rate

$$q_{x,y} = \frac{i_{x,y}}{(\rho_s - \rho)gN}$$

where N is the volumetric sediment concentration ($N=0.60$) and ρ_s, ρ the sediment and water densities respectively. The terms i_x, i_y correspond to the transport rates (Baillard, 1981)

$$i_x = \left\langle \left[\frac{\varepsilon_b}{\tan \phi} \left(\frac{u_o}{u_{ot}} + \frac{d_x}{\tan \phi} \right) \omega_b + \varepsilon_s \frac{u_{ot}}{w} \left(\frac{u_o}{u_{ot}} + \varepsilon_s d_x \frac{u_{ot}}{w} \right) \omega_t \right] \right\rangle$$

$$i_y = \left\langle \left[\frac{\varepsilon_b}{\tan \phi} \left(\frac{v_o}{u_{ot}} + \frac{d_y}{\tan \phi} \right) \omega_b + \varepsilon_s \frac{u_{ot}}{w} \left(\frac{v_o}{u_{ot}} + \varepsilon_s d_y \frac{u_{ot}}{w} \right) \omega_t \right] \right\rangle$$

where $\langle \rangle$ indicates time averaging over the wave period, w is the grain settlement velocity, ϕ the angle of the sediment grains internal friction, u_o, v_o the current velocity near the seabed, d_x, d_y the seabed slope in x, y directions respectively, and u_{ot}, ω_b are given from the formulas

$$u_{ot} = \sqrt{u_o^2 + v_o^2}$$

$$\omega_b = C_f \rho u_{ot}^3$$

and ω_t is the total rate of energy dissipation (Leont'yev, 1996)

$$\omega_t = \omega_b + D e^{3/2(1-\frac{h}{H})}$$

where H is the wave height (Hrms) and D is the mean dissipation rate of wave energy per unit area.

3. Numerical model

3.1. Finite difference equations

The finite difference scheme is used to solve the partial differential equations. The method is not unconditionally stable when it is applied to the set of two dimensional, vertically averaged flow equations especially in areas of arbitrary bathymetry and irregular boundaries. A time-step limitation is necessary to ensure numerical stability. The Courant number, C_r , has to be lower than 2 in order to achieve stability

$$C_r = \Delta t \sqrt{g h_{max}} \sqrt{\frac{1}{\Delta x^2} + \frac{1}{\Delta y^2}}$$

where Δt is the time-step of the finite-difference scheme, $\Delta x, \Delta y$ the horizontal grid spacing in the x, y directions respectively and h_{max} the maximum water depth of the numerical study area. The discretization of the partial differential equations is as follows

$$\frac{\eta_{i,j}^{n+1} - \eta_{i,j}^n}{\Delta t} = \frac{(U(d+\eta))_{i+1,j}^n - (U(d+\eta))_{i,j}^n}{\Delta x} + \frac{(V(d+\eta))_{i,j+1}^n - (V(d+\eta))_{i,j}^n}{\Delta y} = 0$$

$$\frac{U_{i,j}^{n+1} - U_{i,j}^n}{\Delta t} + U_{i,j}^n \frac{U_{i+1,j}^n - U_{i-1,j}^n}{2\Delta x} + V_{i,j}^n \frac{U_{i,j+1}^n - U_{i,j-1}^n}{2\Delta y} + g \frac{\eta_{i,j}^{n+1} - \eta_{i-1,j}^{n+1}}{\Delta x} = v_h \frac{U_{i+1,j}^n - 2U_{i,j}^n + U_{i-1,j}^n}{\Delta x^2} + v_h \frac{U_{i,j+1}^n - 2U_{i,j}^n + U_{i,j-1}^n}{\Delta y^2} - \frac{\tau_{sx}^n - \tau_{bx}^n}{\rho h} \left(\frac{S_{xx}^n}{2\Delta x} \right) + \frac{S_{xy}^n}{2\Delta y} \left(\frac{S_{xy}^n}{2\Delta y} \right)$$

and

$$\frac{V_{i,j}^{n+1} - V_{i,j}^n}{\Delta t} + U_{i,j}^n \frac{V_{i+1,j}^n - V_{i-1,j}^n}{2\Delta x} + V_{i,j}^n \frac{V_{i,j+1}^n - V_{i,j-1}^n}{2\Delta y} + g \frac{\eta_{i,j}^{n+1} - \eta_{i,j-1}^{n+1}}{\Delta x} = v_h \frac{V_{i+1,j}^n - 2V_{i,j}^n + V_{i-1,j}^n}{\Delta x^2} + v_h \frac{V_{i,j+1}^n - 2V_{i,j}^n + V_{i,j-1}^n}{\Delta y^2} - \frac{\tau_{sy}^n - \tau_{by}^n}{\rho h} \left(\frac{S_{xy}^n}{2\Delta x} \right) + \frac{S_{yy}^n}{2\Delta y} \left(\frac{S_{yy}^n}{2\Delta y} \right)$$

where $h=d+\eta$.

4. Application to a seabed of smooth geometry

4.1. Detached Breakwaters

The presented model of Aphrodite3D software was applied to a smooth seabed geometry with three detached breakwaters of 75m length, 4m of width and 25m of spacing between them, located at a distance of $X=110m$ from the nearly straight shoreline (perpendicular to the shore). The length of the model area is 3000 m (x-direction) while the width is 500 m (y-direction). The mean seabed slope is $s=0.030$. The wave height and period used for the computations was $H_s=2.30m$ and $T_s=5.80s$, respectively for North-West winds of 7- 8 *Beaufort*. The grain size of the seabed sediments was kept the same for all simulations $D_{50}=0.20mm$. The angle of incoming waves was set at $\alpha=30^\circ$ counter clockwise in respect to the normal to the shoreline. These wave climate conditions were used as input to the coastal simulation model. The coast is subjected to erosion and breakwaters are designed to mitigate erosion at the central part of this coastal region. Three structural option are examined: The type of emerged breakwaters with the crest of the structures at 1m above mean water level (MWL), the type of breakwaters with their crest equal to the MWL and the type of submerged breakwaters with their crest at 0.20m beneath MWL). These structural options as well as wave climate conditions used for the numerical simulations are described in the following table

Table 1. Structural options and wave climate conditions for numerical simulations with breakwaters

Scenario No	Type of Breakwaters	Crest height (m, in respect to the MWL)	Wave height H_s (m)	Wave period T_p (sec)
0	No structures	-	2.30	5.80
1	emerged	+1.0	2.30	5.80
2	Crest at MWL	0.0	2.30	5.80
3	submerged	-0.20	2.30	5.80

In order to extract useful information from the simulation model, discrete scenarios are examined as also shown in Table 1. In scenario No 0 no structures are examined and the model calculate both the hydrodynamic conditions and seabed evolution on the entire length of the coastal area. In scenario No1, numerical simulations are conducted with emerged breakwaters at the center of the coast while in scenario No 2 simulations are conducted with breakwaters with their crest located at the MWL. Finally in scenario No 3 submerged breakwaters are examined in simulations.

For the scenario 0 (no structures) the flow pattern and seabed morphology changes due to the sediment transport show erosion occurring near the shoreline, as expected

under intense climate conditions. The following figures show this model case.

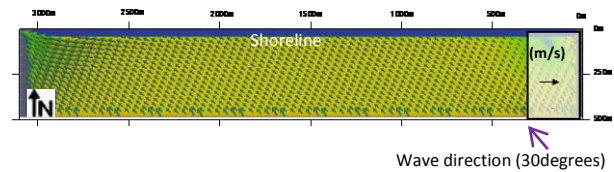


Fig.1 Computational domain and computed nearshore current vectors (high resolution flow model, $H_s=2.30m$, $T_s=5.80s$).

After 20 hours, small changes in seabed morphology for the scenario 0 are predicted. Seabed morphology is presented with topography elevation contours.

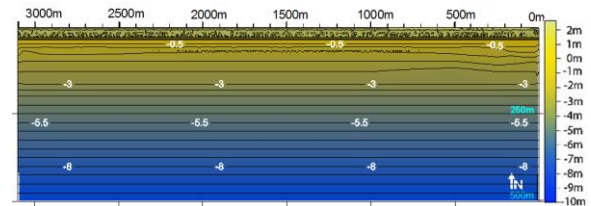


Fig.2 Computed changes in bathymetry after 20 hours for the scenario No 0 (no structures along the coast)

A specific calculation module is enabled to predict seabed evolution in terms of positive (sand accumulation) and negative changes (erosion) in seabed morphology during simulation. These changes can be well presented in a relief map. After calculations for the first scenario 0, negative seabed changes occurred, representing seabed erosion near the shoreline as shown in Fig.3.

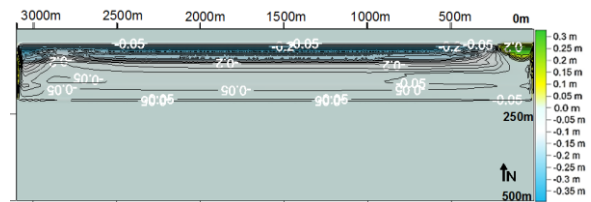


Fig.3 Computed changes in seabed morphology after 20 hours without structures (erosion near shoreline)

Next, scenario No 1 is examined in order to predict bathymetry changes due to the presence of three emerged, detached breakwaters at the center of the coast. High resolution hydrodynamic calculations are executed and the flow pattern of circulating currents near the structures is presented in Figure 4 as calculated after 30 hours. Breakwaters are numbered as also shown in Fig.4

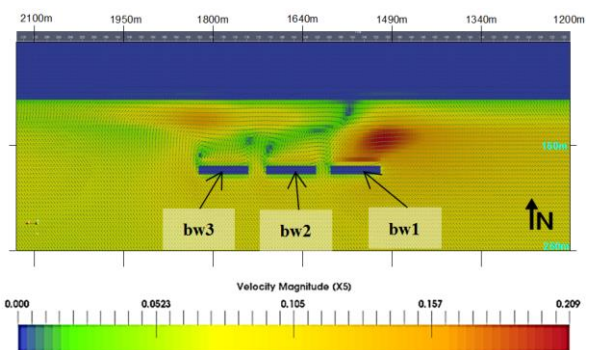


Fig.4 Hydrodynamic flow simulation around emerged, detached breakwaters (part of computational domain, high resolution simulation, velocity magnitude values X5)

After 30 hours, sediment accumulation is observed between initial shoreline and the structures. Seabed rise of $H=0.35\text{m}$ is predicted from the model under these specific conditions behind the first (bw1 - western) breakwater while smaller sediment accumulation is calculated behind next two breakwaters. Out of the structures region, negative values in sediment budget dominate and seabed erosion occurs.

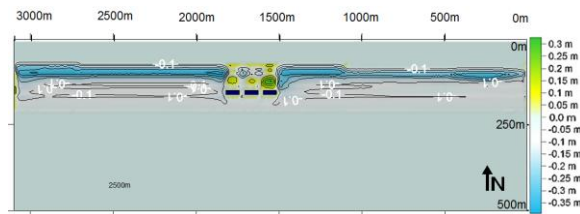


Fig.5 Computed changes in seabed morphology after 30 hours near emerged breakwaters (sediment deposition behind structures. Green area: deposition, Blue area: erosion)

Next, scenario No 2 is examined to predict seabed morphology changes due to the presence of three detached breakwaters at the center part of the coast with their crest located at the mean water level (MWL). Nearshore current circulation is calculated with vortices shaped behind breakwaters as in scenario No 1. The vector field for this simulation is shown in Fig. 6

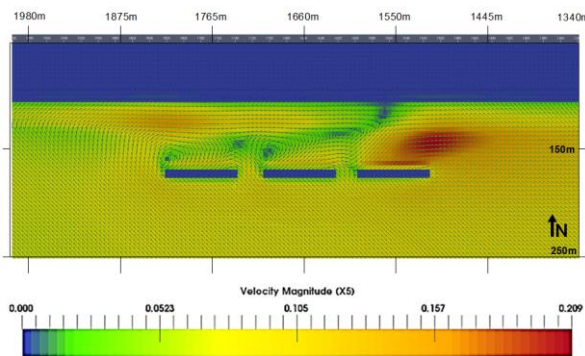


Fig. 6 Vector field near breakwaters with vortices shaped (part of computational domain, high resolution simulation, velocity magnitude values X5)

After 30 hours, the seabed morphology is predicted with sediment accumulation along the area behind the breakwaters. The result of this simulation is shown in Fig. 7

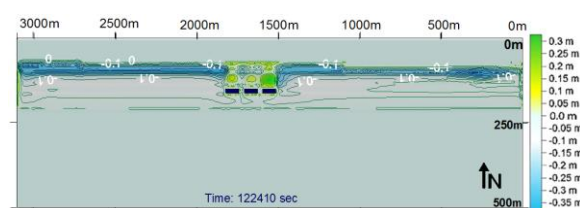


Fig.7 Computed changes in seabed morphology after 30 hours near breakwaters (sediment deposition behind structures. Green area: deposition, Blue area: erosion)

Scenario No 3 follows and the simulation takes in account the limited height of all three breakwaters beneath the sea surface (MWL). The hydrodynamic flow is not severely affected from the presence of submerged structures while the sediment transport and seabed evolution simulation provides significant results. Sediment deposition is much smaller than in the previous two scenarios and it is developed only close to the structures. Therefore higher deposition occurs behind the structures while lower occurs at the front (toe of breakwaters). The result of this simulation is shown in Fig. 8

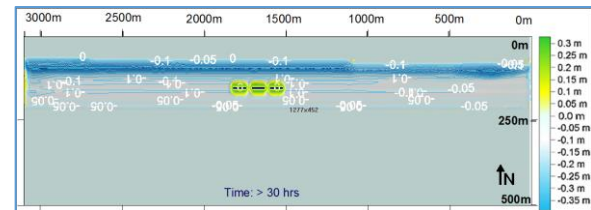


Fig.8 Computed changes in the vicinity of breakwaters in seabed morphology after 30 hours (Green area: higher deposition, Yellow area: lower deposition)

5. Conclusions

In this study a high resolution model of Aphrodite3D Software for predicting the three dimensional (3D) seabed evolution was developed. Different structural scenarios according to different types of breakwaters were adopted and simulations were carried out in these scenarios to investigate the performance of the model. All tests were conducted under storm conditions of duration of several hours on a coastal zone of mild slope. Based on the simulations results, the following conclusions are derived:

Scenario No 0 – no structures along the coast: In this option the simulation predicts sediment transport and erosion of the coast along the shoreline as expected under storm conditions adopted in calculations.

Scenario No 1 – emerged breakwaters: In this option the simulation predicts sediment accumulation between the initial shoreline and the structures. This is a typical result in many coastal applications documented in the coastal engineering literature. A challenging result is the local sediment deposition behind all three emerged breakwaters.

Scenario No 2 – breakwaters crest at MWL: In this option the simulation also predicts sediment accumulation in the protected area behind the structures. As with the previous simulation (scenario No 1) local deposition behind breakwaters occurs as well.

Scenario No 3 – submerged breakwaters: In this option the simulation predicts much smaller sediment deposition in the vicinity of breakwaters. Higher sediment deposition is predicted only close to the structures.

Findings on the model's performance and Future Work
Shoreline evolution is associated with seabed evolution and therefore subjected to high sensitivity at very small

depths shown in results. In order to achieve higher accuracy near the shoreline, a new algorithm will be developed for the Aphrodite3D simulation model. The simulation results qualitatively agree with the expected hydrodynamic conditions and seabed morphology changes of many documented applications in the coastal engineering literature.

References

- Goudas C, Karopoulos Ch, Psarropoulou E (2011). Soft Shore Protection: Evaluation of experimental applications, MEDCOAST 2011, Rhodes Island, Greece.
- Γούδας Κ, Καπόπουλος Χ, Ψαρροπούλου Ε (2009). Προστασία ακτών από διάβρωση μέσω μεταβολής των παράκτιων ρευμάτων σε ροή μόνιμων κλειστών στροβίλων, 9^ο Συμπόσιο Ωκεανογραφίας και αλιείας, Πάτρα.
- Goudas C, Karopoulos Ch, Psarropoulou E (2008). Integrated Coastal Zone Management-The Global Challenge, Chapter 14: Soft Shore Protection: Theory and Practice, Research Publishing, Singapore.
- Goudas C, Karopoulos Ch, Psarropoulou E (2006). The Experience of the University of Patras - INTEREG IIIC BEACHMED-e 'PHASE A Conference', Alexandroupoli, Greece.
- Karopoulos Ch (2013). Hard and Soft Protection Methods on Erosion Control: International Experience, Applications in Greece and Cyprus, Presentation in the Circle of Mediterranean Parliamentarians for Sustainable Development (COMPSUD), Iliia, Greece.
- Καπόπουλος Χ. (2013). Διάβρωση των Ακτών. Επιστημονική Παρουσίαση κατόπιν Ειδικής Πρόσκλησης, Βουλή των Ελλήνων.
- Καπόπουλος Χ., Φαλιέρος Χ., Παλαιολόγου Α. (2011), Διάβρωση των Ακτών, Τεχνικό Επιμελητήριο/ΤΔΕ, Ομάδα Εργασίας.
- Karambas Th. V. (2012) 'Design of detached breakwaters for coastal protection: development and application of an advanced numerical model' Proceedings of the 33rd International Conference on Coastal Engineering 2012, I(33), sediment.115.doi:10.9753/icce.v33.sediment.115
- Karambas Th. V. and Koutitas C. (2002). "Surf and swash zone morphology evolution induced by nonlinear waves". *J. of Waterway, Port, Coastal, and Ocean Eng.*, 102-113